Fazio, A., Folco L., and Langenhorst, F., 2021, Possible shock-induced crystallization of skeletal quartz from supercritical SiO_2-H_2O fluid: A case study of impact melt from Kamil impact crater, Egypt: Geology, https://doi.org/10.1130/G49476.1

SUPPLEMENTAL MATERIAL

Possible shock-induced crystallization of skeletal quartz from supercritical SiO_2-H_2O fluid: A case study of impact melt from Kamil impact crater, Egypt

Agnese Fazio[1], Luigi Folco[2], and Falko Langenhorst[1]

[1]*Analytical Mineralogy of Nano- and Microstructures, Institute of Geosciences, Friedrich Schiller University Jena, Carl-Zeiss-Promenade 10, 07745 Jena, Germany*

[2]*Dipartimento di Scienze della Terra, Università di Pisa, V. S. Maria 53, 56126 Pisa, Italy*

APPENDIX

Analytical methods

Micro-Raman spectra were acquired using a WiTec alpha 300R confocal imaging system (WITec Wissenschaftliche Instrumente und Technologie GmbH, Ulm, Germany). Spectra were acquired using the 531.95 nm emission Nd YAG laser light with 25 mW nominal power at the sample surface and a spot size of 1-2 μm. Spectra were acquired through 50X (0.85 NA) and 100X (0.9 NA) objectives and consisted of 3 to 6 acquisitions with 10 to 30 s integration time. The Raman signal was collected in the spectral interval of 70-1270 cm^{-1} with a spectral resolution of 1.17 cm^{-1} (grating 600 grooves mm^{-1}). Silicon spectra (main peak at 520.5 cm^{-1}) were acquired at the beginning and the end of each micro-Raman session and the acquired spectra were consequently calibrated. The cosmic ray spikes were corrected using the function CCR (filter size = 4; dynamic factor = 4) implemented in the WITec company software Project FOUR. Raman spectra were identified using the RRUFF Database (Lafuente et al., 2015).

A FEI Quanta3D FEG dual beam workstation (FEI Co., Eindhoven, the Netherlands) was employed for the acquisition of the electron images and energy-dispersive X-ray spectroscopy (EDX) analyses and mapping. It was operated with an acceleration voltage of 20 kV and beam current of 4 nA.

During this study, a second thin section was prepared and used for the extraction of electron transparent samples for the transmission electron microscopy (TEM) investigation. Electron transparent samples were prepared via Ar ion milling (Leica EM RES102; Leica Microsystems GmbH, Wetzlar, Germany). This technique was preferred to the focused ion milling (FIB) preparation due to the high porosity of the sample and to obtain larger electron transparent areas in a shorter time. Three-mm copper disks (50 mesh) were glued on the thin section and removed from the support glass. The samples were thinned for ca. 5 hours (4.5 kV and 14°) and polished for ca. 30 minutes (2.5 kV and 14°). Then, the samples were coated with a thin carbon layer (<10 nm). Three samples were investigated by TEM (FEI Tecnai G^2 FEG) operating at 200 kV. Images were acquired with a Gatan UltraScan 2k CCD camera (Gatan Inc., Pleasanton, CA, USA).

Figure Captions

Fig. S1. Overview images of the sample L09, a lapillus made of SiO_2 vesicular glass and relicts of quartz grains. A) Microphotograph of the end cut of the sample. The white areas are quartz crystals. The dark-grey areas are glass. The glass is locally stained by reddish material (Fe-oxides). B) Planar polarized light (PPL) composite microphotograph of one of the two investigated thin sections. The sample consists of SiO_2 vesicular glass with local enrichments of Fe and Al determining variations in the vesicle size and glass color (i.e., the white arrow points a Fe,Al-rich vein). The red circles mark large relicts of quartz grains.

Fig. S2. Planar polarized light image of the possible protolith of the lapillus studied in this work. This image is from a reddish quartz arenite (labelled L07b) collected from a large boulder 90 m due ESE from the crater rim. The grain size varies from medium to very coarse, reddish matrix constitutes up 5 vol% and surrounds almost all quartz grains. The porosity is high, up 24 vol% (Fazio et al., 2014). The maximum length of the largest grain in the image is 2.3 mm. Note the common fluid and mineral inclusions in quartz grains.

Fig. S3. Corresponding crossed polarizers images of the Fig. 1. A) Relict quartz almost completely amorphized and rimmed by unshocked quartz. The reddish color is due to the occurrence of Fe-oxides. B) Skeletal quartz aggregate embedded in a relict quartz. The starts mark six possible nucleation sites.

Figure S4. Backscattered electron SEM (A-C) and bright-field TEM (D) images of the relict quartz grains. They are characterized by small scale domains with PDFs, amorphous silica without vesicles, and amorphous silica with isolated vesicles. A) Zonate contact of the relict quartz with the vesicular glass. At direct contact with the vesicular glass, the relict quartz consists of amorphous silica material without vesicles. Far from the vesicular glass, PDFs are recognizable. This indicates the effect of a T gradient in the amorphization of quartz and the consequent survivor of large relicts. B) Detail of a portion of a relict quartz with isolated vesicles. The portion of the grain close to the vesicles is amorphous, away from the vesicles up to three sets of PDFs are recognizable. C) PDF-rich portion of a quartz relict grain. The crystalline portion (brighter) constitutes ~10% of the image. D) Typical PDF-rich areas of the relict quartz. Two main and two minor sets of PDFs are recognizable (dashed white lines). PDFs have different thicknesses and spacings.

Fig. S5. Selected Raman spectra from impactite L09. A) Weakly shocked quartz. All quartz peaks are well identifiable, although the peaks are shifted towards lower values. The main shift regards the position of the main quartz Raman peak at 462 cm^{-1}, which is related to the vibration of the oxygen atom connecting two silica tetrahedra and interpreted as an increase in the angle spanning two tetrahedra due to the amorphization induced by the shock (Fritz et al., 2011). The contribution of the glass bands is recognizable as a shoulder of the main quartz peak and at the 800 cm^{-1} (see inset). B) Highly shocked quartz. The quartz peaks are clearly superimposed by the glass bands. The shift towards lower Raman values increases. C) Amorphous domain within a quartz relict. Quartz peaks are no longer detected. No variations of the Raman spectra have been detected in vesicle-free and vesicle-bearing areas.

D) Perfectly crystalline quartz from a unshocked (skeletal) quartz aggregate. Quartz from these aggregates is occasionally associated with Fe-oxides, dominantly magnetite (E) and Al-doped magnetite (F; Monarrez-Cordero et al., 2017).

REFERENCES CITED

Fazio, A., Folco, L., D'Orazio, M., Frezzotti, M. L., and Cordier, C., 2014, Shock metamorphism and impact melting in small impact craters on Earth: Evidence from Kamil crater, Egypt: Meteoritics & Planetary Science, v. 49, no. 12, p. 2175-2200.

Fritz, J., Wünnemann, K., Reimold, W. U., Meyer, C., and Hornemann, U., 2011, Shock experiments on quartz targets pre-cooled to 77 K: International Journal of Impact Engineering, v. 38, no. 6, p. 440-445.

Lafuente, B., Downs, R. T., Yang, H., and Stone, N., 2015, 1. The power of databases: The RRUFF project, *in* Thomas, A., and Rosa Micaela, D., eds., Highlights in Mineralogical Crystallography De Gruyter (O), p. 1-30.

Monarrez-Cordero, B. E., Amezaga-Madrid, P., Fuentes-Cobas, L., Montero-Cabrera, M. E., and Miki-Yoshida, M., 2017, High and fast adsorption efficiency of simultaneous As^{+3}, As^{+5} and F^{-} by Al-doped magnetite synthesized via AACVD: Journal of Alloys and Compounds, v. 718, p. 414-424.

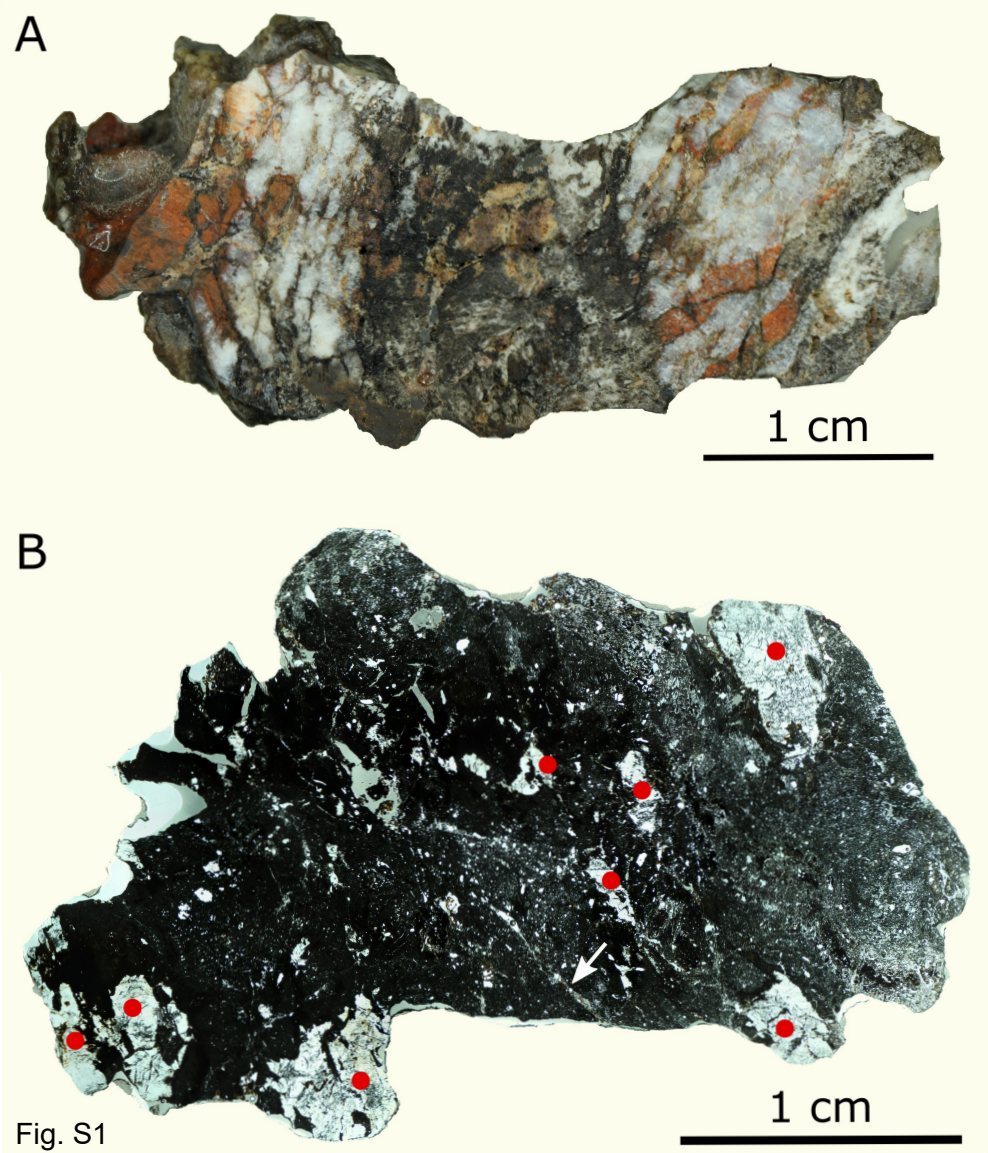

Fig. S1

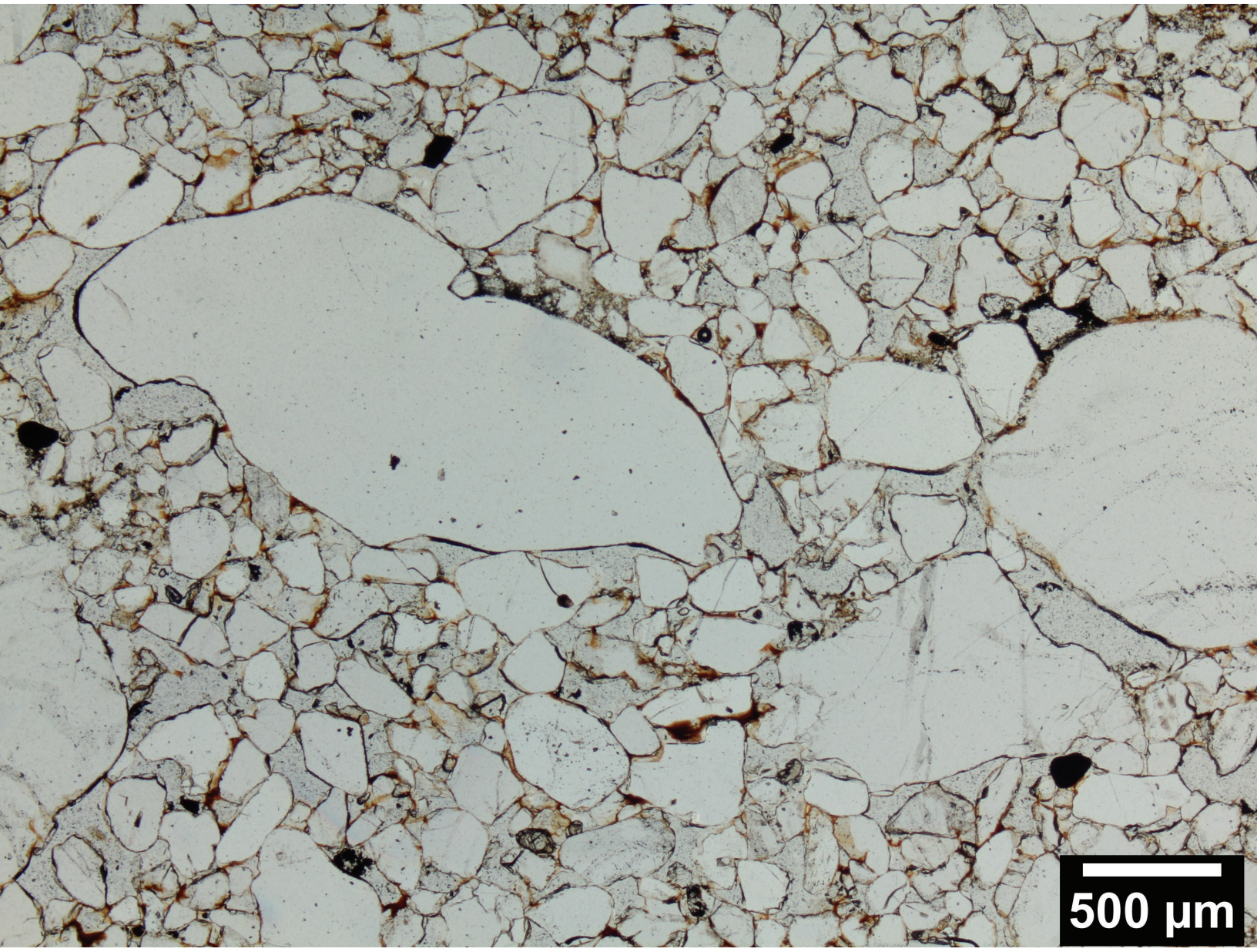

Fig. S2

Fig. S3

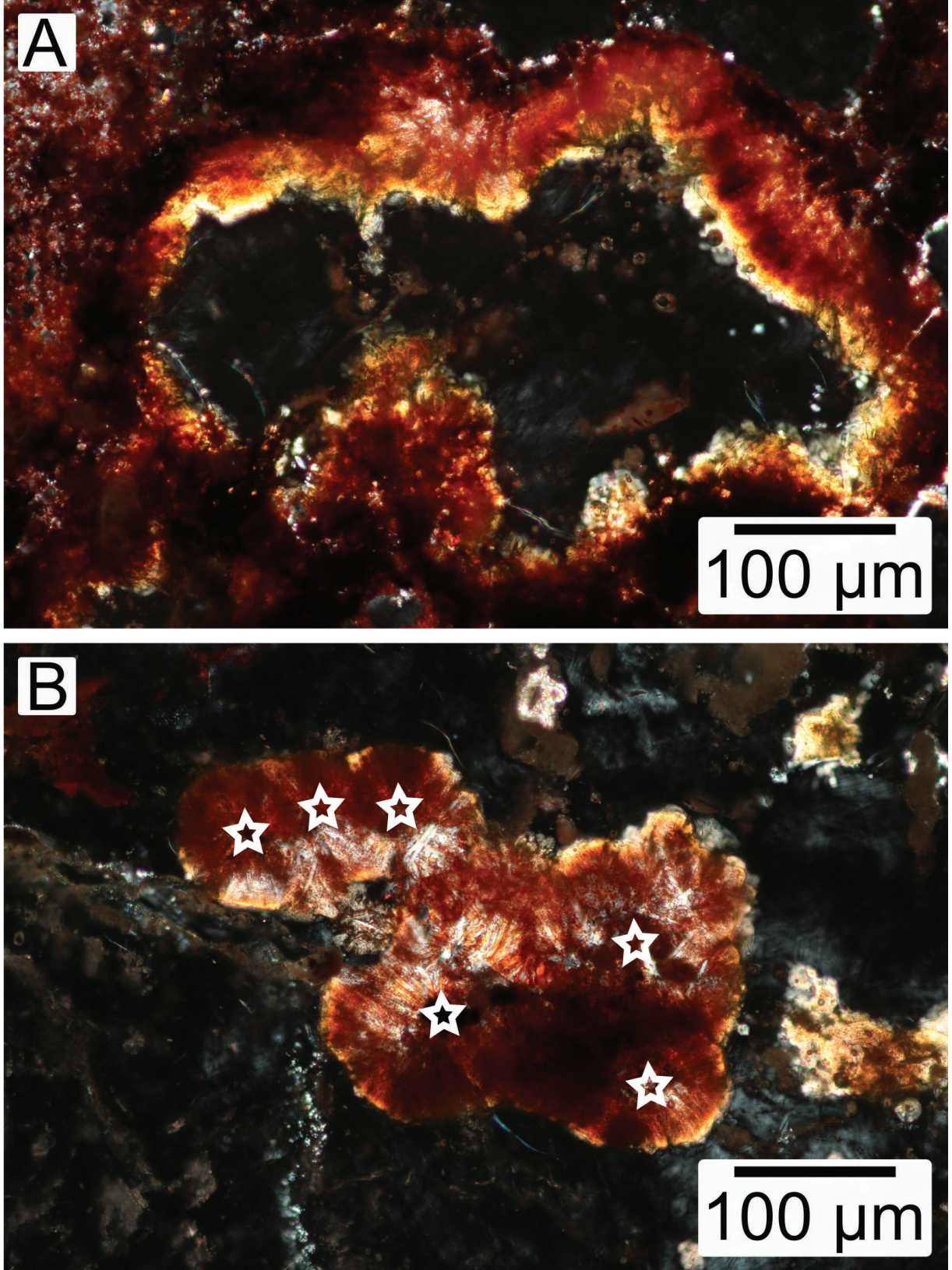

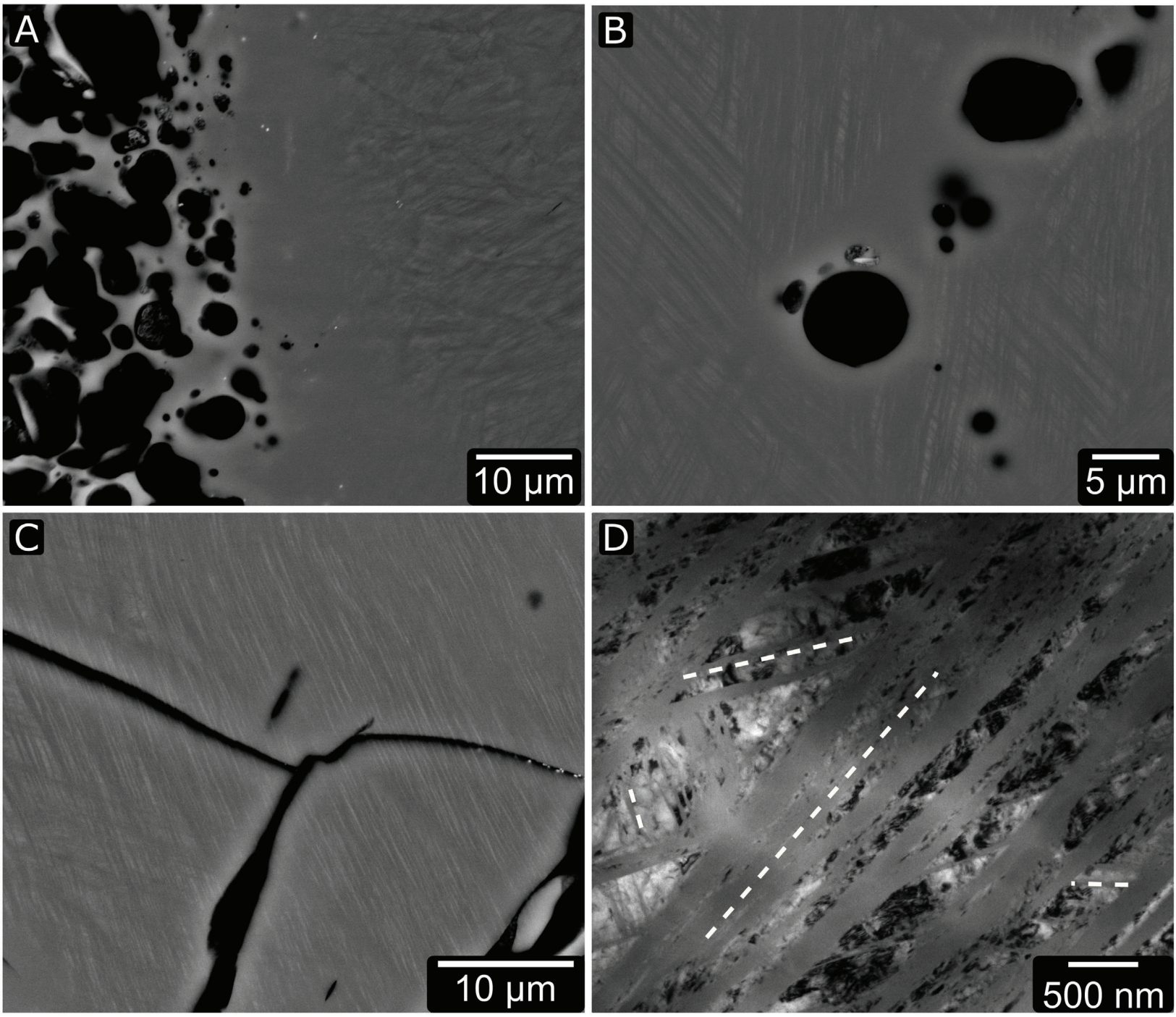

Fig. S4

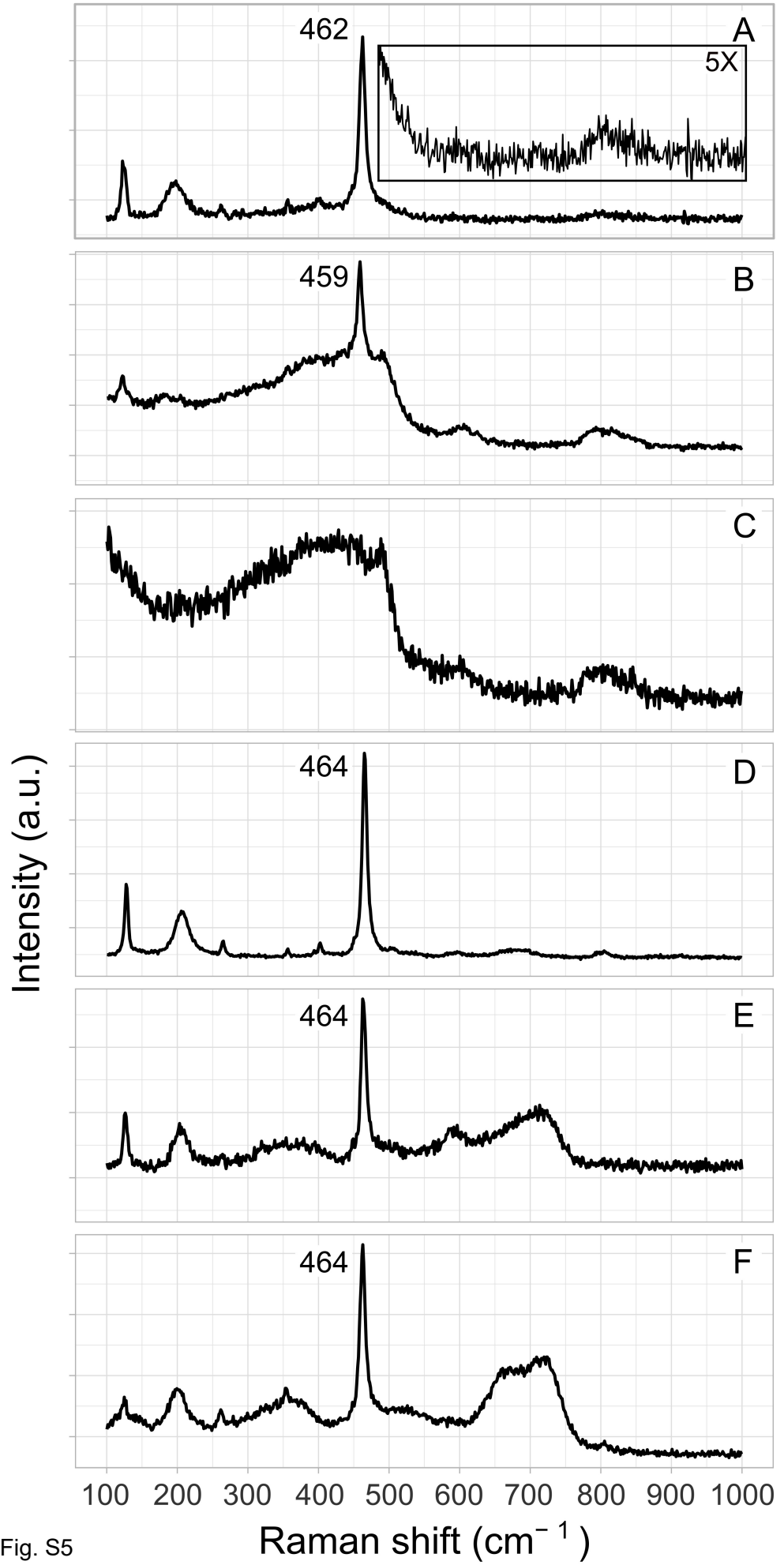
462
A
5X
459
B
C
464
D
464
E
464
F
Intensity (a.u.)
100
200
300
400
500
600
700
800
900
1000
Raman shift (cm^{-1})

Fig. S5